Integration of functional and structural connectivity from rs-fMRI and DTI to study healthy maltreated adolescents

Minhui Ouyang[1], Uma Rao[2], Tejasvi Gundapuneedi[1], and Hao Huang[1]

[1]*Advanced Imaging Research Center, University of Texas Southwestern Medical Center, Dallas, TX, United States,* [2]*Department of Psychiatry and Behavioral Sciences, Meharry Medical College, Nashville, TN, United States*

Target Audience: The psychiatrists, psychologists, neurologists and MR physicists who wish to use advanced MR techniques to detect subtle functional and structural connectivity abnormality in psychiatrically high-risk group such as maltreated adolescents.

Introduction and Purpose: Childhood maltreatment (MALTX), including emotional abuse, physical abuse, sexual abuse and neglect, is widespread in the United States. MALTX has been known to produce long-lasting impairments in behavioral, cognitive and social functioning, but their underlying mechanisms are not well understood. Integrating functional and structural connectivity from resting state fMRI (rs-fMRI) and diffusion tensor imaging (DTI) provides insight of the affected brain circuits including both cortical region and white matter tracts in the maltreated subjects. Recent DTI investigation (1-2) suggests white matter abnormality of maltreated young adults and adolescents. However, to our knowledge, there have been no reports investigating the maltreated group with integrated functional and structural connectivity measures. In this study, 19 MALTX adolescent volunteers and 13 age-matched control volunteers were recruited and underwent both rs-fMRI and DTI scanning. The rs-fMRI and DTI datasets were analyzed to identify the disrupted functional and structural connectivity, respectively. Our aim was to identify the disrupted structural and functional connectivity and reveal the relationship of the abnormal connectivity of both types in the maltreated healthy subjects. The abnormality of the structural and functional connectivity preceding the onset of psychopathology may serve as potential biomarkers of psychiatric disorders such as depression and substance abuse.

Methods

Participants: 19 adolescent volunteers (age=15.9±2.8) with no personal history of a psychiatric illness, but experienced MALTX prior to age 10 years, and 13 adolescent volunteers (age=16.4±3.9) with no personal or family history of a psychiatric disorder or trauma history were recruited. All participants were between 12-20 years, and Tanner Stage III, IV or V of pubertal development. All 32 subjects were scanned with DTI and 19 subjects (9 maltreated and 10 controls) were scanned with rs-fMRI. *rs-fMRI and DTI acquisition:* A 3T Philips Achieva MR system was used. DTI data were acquired using a single-shot EPI with SENSE. DTI parameters: imaging resolution=2x2x2.2 mm, slice number=65, independent diffusion-weighted directions=30, b-value = 1000 sec/mm^2, repetitions=2. Co-registered rs-fMRI was acquired with a single-shot gradient EPI T_2*-weighted sequence with time series of 240 EPI volumes. Imaging resolution of rs-fMRI is 3.4x3.4x4mm. *rs-fMRI data analysis:* rs-fMRI was processed with AFNI (3). After pre-processing, signals were low-pass filtered with 0.1 Hz cutoff frequency. Seed region of the posterior cingulate cortex (PCC) was centered at (-10, -54, 14) and (8, -54, 14) in Talairach space. The average seed region time course in the filtered data was correlated with all other pixels to form functional connectivity maps for each subject. *DTI data analysis:* TBSS (4) was used for voxel-wise comparison of fractional anisotropy (FA) maps. Different from standard TBSS, the single subject template used for nonlinear registration process in TBSS is identical to the template used for establishing JHU ICBM-DTI-81 (5). *Integrated rs-fMRI and DTI analysis:* The voxels with significant functional connectivity differences were used as region of interest (ROI) to initiate DTI-based tractography The traced white matter tracts were identified with the reference (6). *Clinical correlation:* The mean PCC-PFC correlation values and FA values at disrupted clusters were extracted to be correlated with clinical scores.

Results

Functional connectivity: Fig. 1 shows the functional connectivity within left superior prefrontal cortex (PFC) of the default network for the control and maltreated groups, respectively. Using the threshold of p=0.05 after false discovery rate (FDR) correction, the positive connectivity in both groups was significant between PCC and the PFC. *Associated structural connectivity:* As shown from Fig. 2, part of left superior longitudinal fasciculi (SLF-L), left inferior fronto-occipital fasciculus (IFO-L) and genu of the corpus callosum (GCC) were traced from the voxels where maltreated subjects had less functional connectivity (cluster at cross-hair in Fig. 1). Concurrently, significant white matter disruptions in SLF-L and IFO-L have been found with TBSS analysis of FA measurements in maltreated group, indicating the relationship of the disrupted functional connectivity and disrupted structural connectivity.

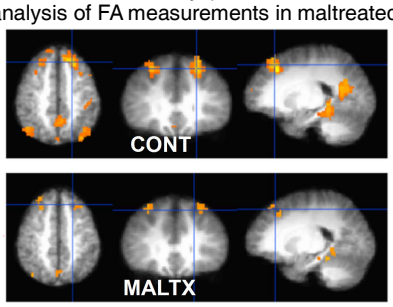

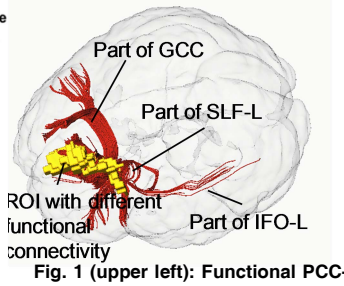

The averaged FA of the two groups in these tracts and correlation coefficient at PFC of the two groups are listed in Table 1. Between the two groups, significant FA differences (p<0.05) can be found in SLF-L and IFO-L while significant correlation coefficient difference (p<0.05) can be found in PFC. *Clinical correlation:* After controlling for age, sex and socioeconomic status, early life adversity correlated negatively with SLF-L (r_{24}=-0.63, p<0.001) and IFO-L (r_{24}=-0.6, p<0.001). Maltreated group had a negative correlation between PFC-PCC connectivity with clinician-rated depressive symptoms (CDRS: r = -0.77; p=0.06). Data from normal controls did not show any significant correlations.

Fig. 1 (upper left): Functional PCC-PFC connectivity map for control and maltreated group. The underlying brain images are average of all subjects in Talairach space. The cross-hair indicates the voxels in left PFC with significant functional connectivity difference.
Fig. 2 (upper right): 3D reconstruction of white matter fibers (red) traced from the rs-fMRI cluster (yellow) at PFC. The red fibers are part of SLF-L, IFO-L and GCC, as indicated by black labels. Yellow cluster is reconstructed from the voxels with significant functional connectivity difference in Fig. 1.
Table 1 (below): The list of structural connectivity differences for the tracts traced from left PFC and functional connectivity difference at left PFC. p values less than 0.05 are bold. See text for abbreviations.

Structural connectivity, FA measurement									Functional connectivity, correlation coefficient		
SLF-L			IFO-L			GCC			PFC		
MALTX	CONT	p	MALTX	CONT	p	MALTX	CONT	p	MALTX	CONT	p
0.34	0.43	**<0.01**	0.39	0.51	**<0.01**	0.489	0.493	0.47	0.123	0.203	**0.030**

Discussion and conclusion

Even before the onset of psychopathology, both functional and structural changes were detected in the maltreated group. Association of structural and functional connectivity has been investigated in multiple reports (e.g. 4-5) by integrating DTI and rs-fMRI in normal subjects. By using the disrupted functional connectivity voxels from AFNI as region of interest (ROI) to initiate fiber tracking, the traced white matter tracts were identified to be consistent to the tracts which have clusters with microstructural abnormality from TBSS analysis. This may be the first study to reveal the consistent structural and functional connectivity abnormality in maltreated group. Both structural and functional connectivity measures showed correlation with clinical scores, suggesting that abnormal structural and functional connectivity measures might serve as potential biomarkers of vulnerability to psychopathology in maltreated subjects. A larger sample size will be needed for statistical power.

References: [1] Choi et al (2009) Biol Psychiatry 65, 227. [2] Huang et al (2012) Neuropsychopharmacology 37, 2693. [3] Cox (1996) Comput Biomed Res 29, 162. [4] Smith et al (2006) NeroImage 31:1487. [5] Mori, S et al (2008) NeuroImage 40: 572. [6] Wakana et al (2004) Radiology 230, 77. [7] Greicius et al (2009) Cereb Cortex 19, 72. [8] Damoiseaux and Greicius (2009) Brain Struct Funct 213, 525. **Acknowledgement:** NIH EB09545, MH092535, DA014037, DA015131, DA017804, DA017805, MH062464, MH068391 and RR003032.